



ELSEVIER

Available online at www.sciencedirect.com

 ScienceDirect

Proceedings of the Combustion Institute 31 (2007) 2721–2729

Proceedings
of the
Combustion
Institute

www.elsevier.com/locate/proci

Extinguishment mechanisms of coflow diffusion flames in a cup-burner apparatus

Fumiaki Takahashi ^{a,*}, Gregory T. Linteris ^b, Viswanath R. Katta ^c

^a National Center for Space Exploration Research on Fluids and Combustion, NASA Glenn Research Center, 21000 Brookpark Road, MS 110-3, Cleveland, OH 44135, USA

^b Fire Research Division, National Institute of Standards and Technology, Gaithersburg, MD 20899, USA

^c Innovative Scientific Solutions, Inc., Dayton, OH 45440, USA

Abstract

The extinguishment processes of methane–air coflow diffusion flames formed on a cup burner in earth gravity have been investigated experimentally and computationally. As a gaseous fire-extinguishing agent (CO₂, N₂, He, Ar, CF₃H, CF₃Br, or Br₂) was introduced gradually into a coflowing oxidizer stream, the base (edge) of the flame detached from the burner rim, oscillated, and eventually extinguished. This extinguishment occurred via a blowoff process (in which the flame base drifted downstream) rather than the global chemical extinction typical of counterflow diffusion flames. The agent concentration in the oxidizer required for extinguishment was nearly independent of the mean oxidizer velocity over a wide range, exhibiting a plateau region. Numerical simulations with full chemistry revealed the unsteady blowoff process and predicted the minimum extinguishing concentration (MEC) of each agent in good agreement with the measurement. The calculations indicated that flame stabilization at the flame base depended upon diffusion of radicals and heat from the trailing diffusion flame upstream into the peak reactivity spot (i.e., reaction kernel). For physically acting agents, the flame blew off as the trailing diffusion flame temperature decreased to ≈1700 K, at which point the back-diffusion of heat and chain radicals into the flame stabilizing region was sufficiently reduced. Consequently, the relative ranking of inert agent effectiveness depended primarily on the heat capacity of the agent-laden oxidizer. Nonetheless, for helium, the MEC was lower than that of argon (which has the same specific heat). The numerical results showed that addition of helium leads to greater heat losses from the downstream diffusion region of the flame than addition of argon because helium addition raised the thermal conductivity of the gas mixture relative to argon addition. The results highlight the importance of the downstream diffusion flame conditions for supporting the flame stabilization which ultimately occurs at the reaction kernel.

© 2006 The Combustion Institute. Published by Elsevier Inc. All rights reserved.

Keywords: Fire suppression; Extinguishment; Flame stability; Diffusion flames; Cup burner

1. Introduction

The effectiveness of a gaseous fire-extinguishing agent, typically used in a total flooding fire suppression system, depends on the agent's ability to extinguish a fire at the lowest possible

* Corresponding author. Fax: +1 216 433 3793.

E-mail address: Fumiaki.Takahashi@grc.nasa.gov (F. Takahashi).

concentration. To determine this effectiveness in terrestrial fire safety engineering, the cup-burner method, specified in national and international standards [1], has been most widely used [2–9]. The cup-burner flame is a laminar coflow diffusion flame with a circular fuel source (either a liquid pool or a low-velocity gas jet) inside a co-axial chimney with an oxidizing stream. An agent is generally introduced into the oxidizer stream and the minimum extinguishing concentration (MEC) is determined. The cup-burner flame in some ways resembles a real fire, consisting of flame segments subjected to various strain rates and exhibiting flame flickering and tip separation, that then affect the air and agent entrainment into the flame zone. Moreover, a real fire over condensed materials generally forms a leading flame edge, which plays an important role in flame stabilization, spreading, and suppression. Because of its resemblance to fires, great faith has been placed in the cup-burner MEC values, and many safety codes and design practices are based on them. However, fundamental understanding of the flame extinguishment processes for this device is very limited. Little is known concerning the amount of agent that is transported into various regions of the flame, whether the extinguishment occurs due to global flame extinction or destabilization of the edge diffusion flame, and most importantly, how the extinguishment phenomena in the cup-burner scale to larger fires. Clearly, the understanding of fire suppression by chemical inhibitors as well as inert-gas agents would be greatly improved if their effect in cup-burner flames was investigated from a fundamental perspective.

The overall objectives of the present study are to understand the physical and chemical processes of cup-burner flame extinguishment and to provide rigorous testing of numerical models, which include detailed chemistry and radiation sub-models. In previous papers [10–17], flame suppression characteristics of CO_2 , CF_3H , and metallic compound were investigated. This paper reports the experimental and computational results of the extinguishment of methane flames using various gaseous agents (CO_2 , N_2 , He, Ar, CF_3H , CF_3Br , or Br_2). The extinguishment mechanisms for the former four are presented herein and those for the latter three are discussed elsewhere [13,17].

2. Experimental procedures

The cup burner, described previously [6], consists of a cylindrical glass cup (28 mm outer diameter, 45°-chamfered inside burner rim) positioned inside a glass chimney (8.5 cm or 9.5 cm inner diameter, 53.3 cm height). To provide uniform flow, 6 mm glass beads fill the base of the chimney, and 3 mm glass beads (with two 15.8 mesh/cm

screens on top) fill the fuel cup. Gas flows were measured by mass flow controllers (Sierra 860¹) which were calibrated so that their uncertainty is 2% of indicated flow. The burner rim temperature, measured at 3.7 mm below the exit using a surface temperature probe after running the burner for ≈ 10 min, was (514 ± 10) K.

The fuel gas used is methane (Matheson UHP, 99.9%), and the agents are carbon dioxide (Airgas, 99.5%), nitrogen (boil-off), helium (MG Ind., 99.95%), argon (MG Ind., 99.996%), CF_3H (Dupont, 99%), CF_3Br (Great Lakes), and Br_2 (Aldrich, 99.5%). The air is house compressed air (filtered and dried) which is additionally cleaned by passing it through a 0.01 μm filter, a carbon filter, and a desiccant bed to remove small aerosols, organic vapors, and water vapor. To determine the suppression condition, for a fixed mean fuel velocity of 0.92 cm/s, the agent is added (in increments of <1% near extinguishment) to coflowing air (held at a constant flow rate) to decrease the oxygen concentration until extinguishment occurred. The test was repeated at least three times at each of the different coflow velocities.

An uncertainty analysis was performed, consisting of calculation of individual uncertainty components and root mean square summation of components. All uncertainties are reported as *expanded uncertainties*: $X \pm ku_c$, from a combined standard uncertainty (estimated standard deviation) u_c , and a coverage factor $k=2$. Likewise, when reported, the relative uncertainty is ku/X . The expanded relative uncertainties for the experimentally determined quantities in this study are 4% for the volume fractions of Ar, He, N_2 , CO_2 , and 7% for those of CF_3H , CF_3Br , and Br_2 .

3. Computational methods

Unsteady computations of the cup-burner flames were performed using a numerical code (UNICORN), developed by Katta [18] and described in detail elsewhere [13]. A detailed reaction mechanism of GRI-V1.2 [19] for methane–oxygen combustion (31 species and 346 elementary reactions) and NIST CKMech [20] for fluoromethane and bromine inhibition reactions for CF_3H , CF_3Br , and Br_2 (total of up to 92 species and 1644 elementary reactions) are incorporated into UNICORN. A simple, optically thin-media, radiative heat-loss model [21] for CO_2 , H_2O , CH_4 , and CO, was incorporated into

¹ Certain commercial equipment, instruments, or materials are identified in this paper to adequately specify the procedure. Such identification does not imply recommendation or endorsement by NIST or NASA, nor does it imply that the materials or equipment are necessarily the best available for the intended use.

the energy equation. The finite-difference forms of the momentum equations are obtained using an implicit QUICKEST scheme [22], and those of the species and energy equations are obtained using a hybrid scheme of upwind and central differencing.

Calculations are made on a physical domain of 200 mm by 47.5 mm using a 251×101 or 541×251 non-uniform grid system that yielded 0.2 mm by 0.2 mm or 0.05 mm by 0.05 mm minimum grid spacing, respectively, in both the z and r directions in the flame zone. The computational domain is bounded by the axis of symmetry and a chimney wall boundary in the radial direction and by the inflow and outflow boundaries in the axial direction. The outflow boundary in z direction is located sufficiently far from the burner exit (≈ 15 fuel-cup radii) such that propagation of boundary-induced disturbances into the region of interest is minimal. The burner outer diameter is 28 mm and the chimney inner diameter is 95 mm. The burner wall (1-mm long and 1-mm thick tube) temperature is set at 600 K. The mean fuel and oxidizer velocities are 0.921 cm/s and 10.7 cm/s, respectively.

4. Results and discussion

4.1. Visual observations

Figure 1 shows video images of methane–air coflow diffusion flames in a cup-burner apparatus. For the stable flame in air (Fig. 1a), the blue flame base anchored at the burner rim with an inward inclination as a result of the buoyancy-induced flow. The color of the flame zone turned orange-yellow downstream due to soot formation. The flame was flickering at ≈ 11 Hz [10,11] due to instabilities in the buoyancy-induced flow near the flame zone. As an inert fire-extinguishing

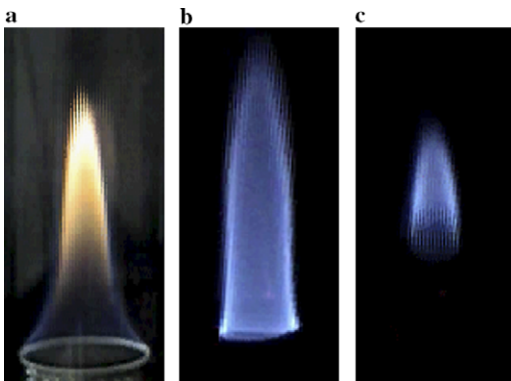


Fig. 1. Methane diffusion flames on a cup burner. $U_f = 0.92$ cm/s, $U_{ox} = 10.7$ cm/s. (a) In air; (b and c) with CO_2 , $X_a \approx 0.158$.

agent was added into coflowing air, the entire flame zone turned blue, and the flame base detached from the burner rim in search of a new stabilization point downstream (i.e., the inward and upward direction). As the agent concentration approached to the extinguishment limit, the flame base oscillated (Fig. 1b) over several millimeters along the streamline direction [16]. As the flame base reached a certain farther location, it was unable to restabilize on the burner rim and thus blew off (Fig. 1c).

4.2. Extinguishment limits

Figure 2 shows for various fire-extinguishing agents the measured ($X_{a,exp}$) and calculated ($X_{a,cal}$) critical agent volume fractions in the oxidizer at extinguishment. These are commonly referred to as the minimum extinguishing concentration (MEC). The measured critical agent volume fractions were nearly independent of the mean oxidizer velocity (U_{ox}) over a wide range for all agents except He, for which $X_{a,exp}$ decreased mildly with increasing U_{ox} . The insensitivity of the extinguishment limit to the oxidizer flow (plateau region), once a minimum flow is achieved, has been reported in the literature [1,5,7]. The fuel velocity, fuel-cup diameter, and chimney diameter are also known to have a small or negligible impact on the agent concentration at suppression [5].

In the plateau region for CO_2 , the data points obtained using the standard glass burner (\square) were consistent with those obtained with a stainless-steel burner (\circ) with a sufficient preheating period [15]. As the oxidizer velocity was decreased below the lower edge of the plateau region in Fig. 2 and approached a threshold ($U_{ox} \approx 1$ cm/s) for form-

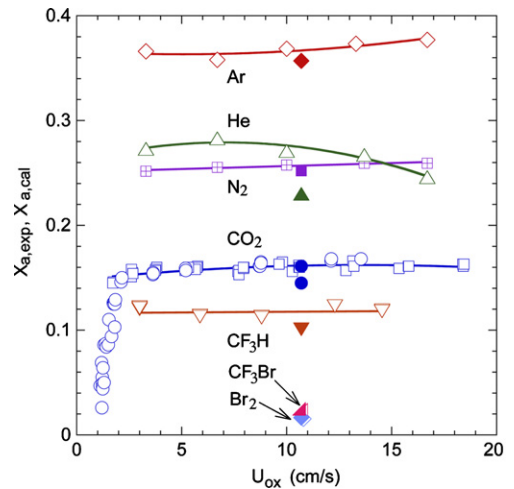


Fig. 2. Measured and calculated critical agent volume fractions at extinguishment.

ing an over-ventilated flame, $X_{a,exp}$ decreased rapidly toward zero. Thus, an under-ventilated flame in $U_{ox} < 1$ cm/s could not be stabilized on the burner.

Table 1 summarizes the measured and calculated minimum extinguishing concentration (MEC), expressed as volume fraction ($X_{a,exp}$ and $X_{a,cal}$). Table 1 also includes the corresponding limiting oxygen volume fractions ($X_{O_2,exp}$ and $X_{O_2,cal}$), the heat capacity of the oxidizer at 298.15 K ($C_{p,ox}$) [23], and the calculated adiabatic flame temperature (T_f) [24] of the stoichiometric methane–air mixture at the measured extinguishing condition for various agents. The limiting oxygen index (expressed in the volume fraction) at extinguishment was determined from the extinguishing agent volume fraction by $X_{O_2} = X_{O_2,initial} (1 - X_a)$, where $X_{O_2,initial}$ = the initial oxygen volume fraction in the oxidizer without agent (0.2095 for air). The MEC value for Br_2 was the lowest (most effective) and that for Ar was highest (least effective). Thus, the relative ranking of the agent effectiveness is:

$Br_2 > CF_3Br > CF_3H > CO_2 > N_2 \approx He > Ar$.

The predicted MEC values at a fixed oxidizer velocity ($U_{ox} = 10.7$ cm/s) were about 6% less than the measured values. The good agreement between the measured and predicted values of the minimum extinguishing concentrations for various agents implies that the complex interactions of the detailed chemical kinetics, the flow field, and the dynamic flame behavior associated with the blowoff process were treated accurately in the numerical model.

Adding an agent has three global effects: diluting the mixture, varying the heat capacity of the mixture, and (for chemically acting agents) changing the heat release per unit mass of oxidizer (due to reaction of the agent itself). Figure 3a shows the heat capacity of the oxidizer stream. For physically acting agents (CO_2 , N_2 , He, and Ar), which act via dilution and heat capacity effects, the agent effectiveness ranking should be essentially that of the agent heat capacity. If heat capacity and dilu-

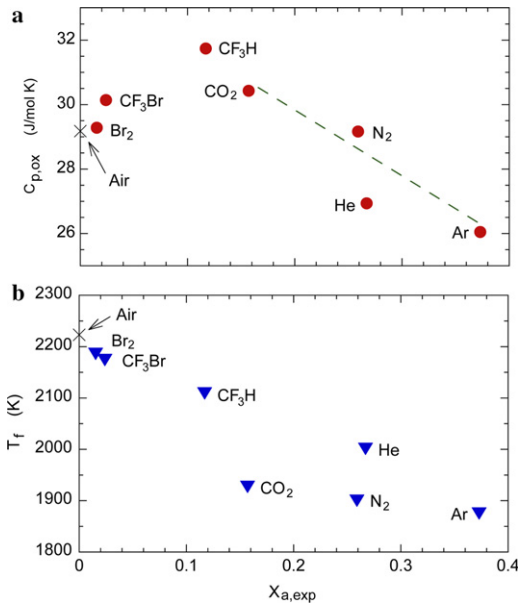


Fig. 3. (a) Heat capacity of the oxidizer and (b) adiabatic flame temperature at the measured extinguishing volume fraction.

tion were the only effects, the points for the oxidizer heat capacity vs. X_a would lie on a straight line (as shown in the figure as a least-squares fit to the points for CO_2 , N_2 , and Ar).

An alternative way to view the data, shown in Fig. 3b, is the calculated adiabatic flame temperature, which simultaneously accounts for dilution, heat capacity changes, and heat release from the inhibitor reaction. In Fig. 3b, the adiabatic flame temperature is shown for a stoichiometric mixture of methane with the oxidizer at the measured extinguishing limit ($X_{a,exp}$). Adding one of the physically acting agents except helium reduced T_f (at the extinguishment point) to about 1900 K as compared to 2223 K for air. In contrast, adding He, CF_3H , CF_3Br , and Br_2 yielded a higher T_f at the extinguishment condition (>2000 K), suggest-

Table 1
Extinguishment limit, heat capacity, and adiabatic flame temperature

| Agent | $X_{a,exp}$ | $X_{a,cal}$ | $X_{O_2,exp}$ | $X_{O_2,cal}$ | $\frac{(X_{a,cal} - X_{a,exp})}{X_{a,exp}}$ | $C_{p,ox}$ at $X_{a,exp}$ (J/mol K) | T_f (K) at $X_{a,exp}$ |
|----------|--------------------|--------------------|---------------------|--------------------|---|-------------------------------------|--------------------------|
| Ar | 0.373 ± 0.015 | 0.357 | 0.131 ± 0.003 | 0.135 | -0.043 | 26.05 | 1875 |
| He | 0.267 ± 0.011 | 0.222 | 0.154 ± 0.002 | 0.163 | -0.169 | 26.94 | 2001 |
| N_2 | 0.259 ± 0.01 | 0.252 | 0.155 ± 0.002 | 0.157 | -0.027 | 29.16 | 1900 |
| CO_2 | 0.157 ± 0.006 | 0.145 | 0.177 ± 0.001 | 0.180 | -0.076 | 30.43 | 1927 |
| | | 0.161 ^a | | 0.176 ^a | 0.025 | | |
| CF_3H | 0.117 ± 0.008 | 0.101 | 0.185 ± 0.002 | 0.189 | -0.137 | 31.74 | 2109 |
| CF_3Br | 0.024 ± 0.001 | 0.0249 | 0.2045 ± 0.0002 | 0.2043 | 0.037 | 30.14 | 2174 |
| Br_2 | 0.0154 ± 0.001 | 0.0167 | 0.2063 ± 0.0002 | 0.2060 | 0.084 | 29.28 | 2186 |

^a Using different kinetic parameters [25] for a methyl-H atom reaction step.

ing that these agents show flame-inhibiting effects beyond those due to dilution and heat capacity. For CF_3H , the chemical inhibition by removal of chain radicals via formation of HF has been reported previously [13]. For Br_2 and CF_3Br , the MEC values ($X_{a,\text{exp}}$ in Fig. 3) are an order-of-magnitude smaller than those of CF_3H and of the inert agents, and an analysis of the catalytic radical scavenging mechanism is in progress [17]. For helium, the numerical results in the next section will explain the reason for its much lower $X_{a,\text{exp}}$ as compared to argon, (which is surprising since they have the same specific heat [$5/2 R$, R : universal gas constant]).

4.3. Structure of the flame stabilizing region

The inner structure of the flame attachment region, revealed by the numerical simulation, provides more detailed physical and chemical insights into the extinguishment processes. Figure 4a shows the calculated structure of methane flames in air, and Fig. 4b that in air with CO_2 at $X_a = 0.143$. The inflow boundary is at $z = -1$ mm and the burner rim is shown in solid black. The variables include, on the right half: velocity vectors (\mathbf{v}), isotherms (T), total heat-release rate (\dot{q}), and the local equivalence ratio (ϕ_{local}); on the left half: the total molar flux vectors of atomic hydrogen (\mathbf{M}_H), oxygen mole fraction (X_{O_2}), oxygen-consumption rate ($-\dot{\omega}_{\text{O}_2}$), and mixture fraction (ξ), including stoichiometry ($\xi_{\text{st}} = 0.055$ [$X_a = 0$] and 0.044 [$X_a = 0.143$]). The local equivalence ratio is defined [26] by considering a stoichiometric expression for intermediate species in the mixture to be converted to CO_2 and H_2O and is identical to the conventional equivalence ratio in the unburned fuel–air mixture. The mixture fraction was determined by the element mass fractions of carbon, hydrogen, and oxygen as defined by Bilger [27].

The common features for the burner-rim-attached flame (Fig. 4a) and the detached flame (Fig. 4b) are as follows. The velocity vectors show the longitudinal acceleration in the hot zone due to buoyancy. As a result of the continuity of the fluid, surrounding air was entrained into the lower part of the flame. The entrainment flow inclined inwardly as a result of the overall stream-tube (streamline spacing) shrinkage due to the significantly low velocity of the fuel compared to that of the oxidizer as well as the flow acceleration downstream. Both the heat-release rate and the oxygen-consumption rate contours showed a peak reactivity spot (i.e., the reaction kernel [28]) at the flame base, where the oxygen-rich entrainment flow crossed the flame sheet, thus enhancing convective (and diffusive) contributions to the oxygen flux. On the other hand, chain radical species, particularly the H atom, diffuse back against the oxygen-rich

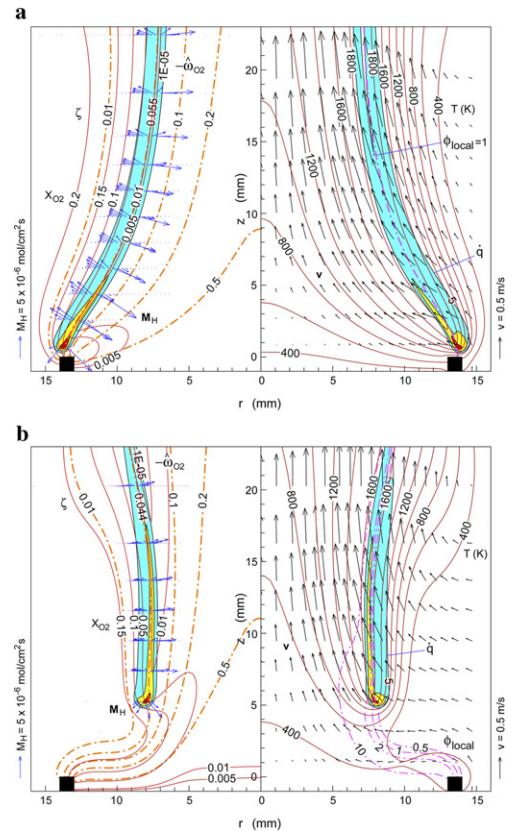


Fig. 4. Calculated structure of methane flames. $U_f = 0.92$ cm/s, $U_{\text{ox}} = 10.7$ cm/s. \dot{q} contours: 5, 20, and 80 J/cm 3 s; $-\dot{\omega}_{\text{O}_2}$ contours: 1×10^{-5} , 5×10^{-5} , and 2×10^{-4} mol/cm 3 s. (a) In air, (b) in air with CO_2 , $X_a = 0.143$.

incoming flow at the flame base (edge). As a result, chain-branching ($\text{H} + \text{O}_2 \rightarrow \text{OH} + \text{O}$) and subsequent exothermic reactions are enhanced particularly at the flame base, thus forming the reaction kernel.

The heat-release rate, oxygen-consumption rate, velocity, temperature, oxygen mole fraction, local equivalence ratio, and mixture fraction at the reaction kernel in the attached flame (Fig. 4a) were: $\dot{q}_k = 155$ J/cm 3 s, $-\dot{\omega}_{\text{O}_2,k} = 0.00041$ mol/cm 3 s, $|\mathbf{v}_k| = 0.275$ m/s $T_k = 1505$ K, $X_{\text{O}_2,k} = 0.041$, $\phi_{\text{local},k} = 0.85$, and $\xi_k = 0.052$, respectively, and in the detached flame (Fig. 4b): $\dot{q}_k = 109$ J/cm 3 s, $-\dot{\omega}_{\text{O}_2,k} = 0.00030$ mol/cm 3 s, $|\mathbf{v}_k| = 0.340$ m/s $T_k = 1459$ K, $X_{\text{O}_2,k} = 0.045$, $\phi_{\text{local},k} = 0.67$, and $\xi_k = 0.039$. In the detached flame, the magnitude of the H atom molar flux vectors decreased and the peak reactivity decreased substantially. The structure of the near-extinguishing flames in air with other inert agents (not shown) resembled that in Fig. 4b.

Figure 5 shows the variations of the calculated temperature, heat-release rate, radiative heat losses, and velocity components along the flame zone (the maximum heat-release rate envelope) in the flames in air and air with various physically acting agents at near-extinguishment concentrations. For all cases, the heat-release rate showed a sharp peak (the reaction kernel) and decreased dramatically in the trailing diffusion flame downstream. Thus, a downstream portion of the flame zone with lower reactivity was supported consequently by an upstream portion with the reaction kernel as the initiating region, as described in detail previously [28]. This is also illustrated by the steep temperature gradient along the flame sheet (Fig. 5a) and the even steeper gradient of H, OH, and O radical volume fraction (not shown). The axial velocity component (U) increased significantly downstream by a cumulative effect of the buoyancy-induced flow. A decrease in the axial velocity component downstream ($z > 18$ mm) for CO_2 was due to the buoyancy-induced vortex (as inferred from a bulge in T , ξ , X_{O_2} contours in Fig. 4b), which squeezed (to cause higher veloci-

ties) and bulged out (lower velocities) the flame zone [10]. The shift in U for helium is due to its larger stand-off distance near extinguishment. For all cases, the temperature at the reaction kernel did not vary much (approximately 1460–1500 K). Without agent, the maximum flame temperature in the trailing diffusion flame (T_{max}) was 1895 K, which was ≈ 300 K lower than the calculated adiabatic flame temperature due to heat losses, oxygen leakage through the flame, and other effects. With an addition of the inert agents near extinguishment, however, T_{max} decreased to a nearly constant value of ≈ 1700 K, as discussed in detail below. The radiative heat losses were largest for added CO_2 , exceeding that for the flame in air, even with its higher flame temperature. Note, however, that while the flames with added inert are blue (non-sooting), the flames without agent produce soot, which is not included in the present radiation model. Nonetheless, the radiative heat losses for the flame in air are not the subject of this investigation, and those for the inhibited flames were significant only where the heat-release rate was comparably small (in the flame-tip region or in zero gravity [14,15]).

4.4. Extinguishment mechanisms

Figure 6 shows the effect of the agent volume fraction on various calculated reaction-kernel properties: the axial and radial stand-off distance from the outer edge of the burner rim (z_k , $y_k = r_k - 14$, r_k : the radius), the total velocity ($|\mathbf{v}_k|$), the temperature at the reaction kernel (T_k), the maximum temperature in the trailing flame (T_{max}), and the heat-release rate (\dot{q}_k). As the agent volume fraction was increased, the reaction kernel gradually moved inward (decreasing y_k) and upward (increasing z_k) and oscillated (a scatter in the z_k and y_k data points) [16] prior to extinguishment. The total velocity and temperature at the reaction kernel were approximately 0.3 m/s and 1500 K, and their variations were moderate (except for the velocity during oscillations). The maximum flame temperature decreased monotonically with X_a (due to dilution and $C_{p,\text{ox}}$ effects) to approximately 1700 K, around which the flame detached, oscillated, and then extinguished (dashed lines in Fig. 6c). The maximum temperature decreased with increasing X_a at a greater rate for helium than argon because, as Fig. 7 shows, the thermal conductivity (and Lewis numbers) of the gas mixture were much larger with helium addition, causing greater heat dissipation. Consequently, the MEC value for He was lower than Ar in spite of the same specific heat. Since the agent in the oxidizer stream reaches the reaction kernel primarily by convection, preferential diffusion is unlikely to play a significant role in the extinguishment processes.

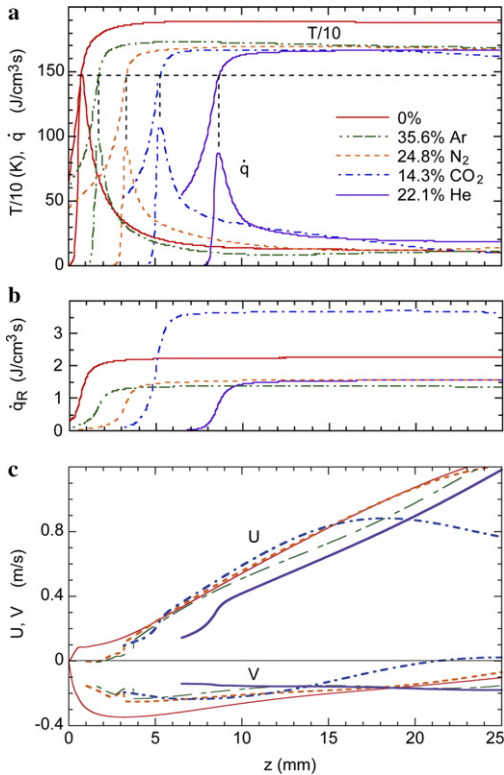


Fig. 5. Calculated (a) temperature, heat-release rate, (b) radiative heat losses, and (c) axial and radial velocity components along the flame zone. $U_f = 0.92$ cm/s, $U_{\text{ox}} = 10.7$ cm/s.

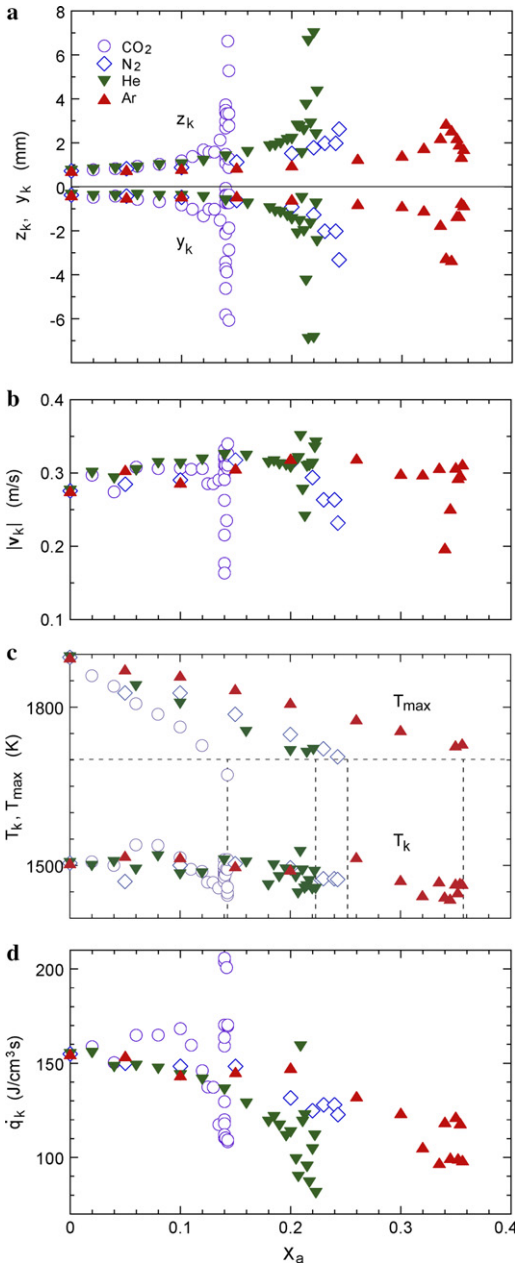


Fig. 6. Effects of agent volume fraction on the reaction-kernel properties and the maximum flame temperature.

Although extinguishment occurred for the inert agents when $T_{\max} \approx 1700$ K, this temperature is much higher than one would expect for a true, low-strain, kinetic flame extinction. For example, cup-burner flames simulated in zero gravity had a flame extinction temperature of about 1300 K [15]. For the present flames, addition of the inert agents caused the heat-release rate (\dot{q}_k) at the reaction kernel to decrease to 80–120 J/cm³ s at extinguishment, but which should still be sufficient to

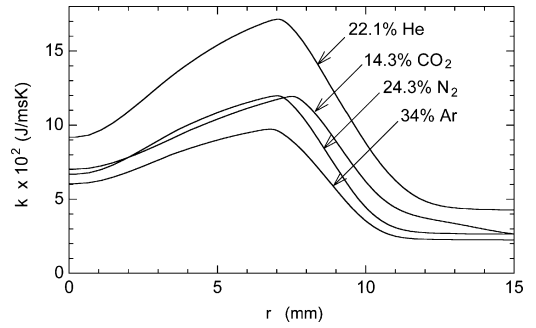


Fig. 7. Thermal conductivity of the gas mixture in methane flames in air with various agents. $z = z_k + 10$ mm.

hold the trailing diffusion flame. Nonetheless, the reaction kernel is dependent upon the flux of both heat and chain radicals from the trailing diffusion flame. Since radical branching reactions are highly temperature dependent, the lower temperature in the trailing flame caused by inert addition was sufficient to reduce the radical flux below that necessary to support the reaction kernel (see the molar flux vectors of H in Fig. 4). As a result, the reaction kernel became weaker and more susceptible to momentary velocity increase due to buoyancy-induced vortex evolution, thus triggering oscillation [16] and, if it failed, leading to blowoff.

5. Conclusions

A fundamental aspect of cup-burner flame extinguishment processes in normal gravity has been studied by the systematic experiments and numerical simulations with full chemistry. Unlike many typical flame extinction processes, in which exothermic chemical reactions shut off, the cup-burner flame extinguishment occurs as a result of a series of flame destabilization processes, i.e., the flame base detachment, drifting, oscillation, and blowoff. For physically acting agents, the flame destabilization occurs as the maximum flame temperature of the trailing diffusion flame decreased to a threshold (≈ 1700 K), thus reducing the radical back-diffusion into the reaction kernel. Therefore, the effectiveness ranking for physically acting agents is essentially that of the oxidizer heat capacity. On the other hand, helium increases the thermal conductivity of the gas mixture significantly and thus cools off the reaction zone of the trailing diffusion flame more effectively than other agents, thus resulting in a lower MEC than that of argon, which has the same specific heat. An understanding of these physical processes in cup-burner extinguishment should prove useful for extrapolating the cup-burner extinguishment values, so widely used by industry, to the fire suppressant needs for full-scale fires.

Acknowledgments

This work was supported by the Office of Biological and Physical Research, National Aeronautics and Space Administration, Washington, DC.

References

- [1] Anon., *Standard on Clean Agent Fire Extinguishing Systems*, National Fire Protection Association, NFPA 2001, Quincy, MA, 2000.
- [2] S.N. Bajpai, *J. Fire Flammability* 5 (1974) 255.
- [3] R. Hirst, K. Booth, *Fire Technol.* 13 (1977) 4.
- [4] R.S. Sheinson, J.E. Pender-Hahn, D. Indritz, *Fire Safety J.* 15 (1989) 437–450.
- [5] A. Hamins, G. Gmurczyk, W. Grosshandler, R.G. Rehwoldt, I. Vazquez, T. Cleary, C. Presser, K. Seshadri, in: W.L. Grosshandler, R.G. Gann, W.M. Pitts (Eds.), *Evaluation of Alternative In-Flight Fire Suppressants for Full-Scale Testing in Simulated Aircraft Engine Nacelles and Dry Bays*. NIST SP 861, National Institute of Standards and Technology, 1994, pp. 345–465.
- [6] G.T. Linteris, G.W. Gmurczyk, in: R.G. Gann (Ed.), *Fire Suppression System Performance of Alternative Agents in Aircraft Engine and Dry Bay Laboratory Simulations*. NIST SP 890: vol. II, National Institute of Standards and Technology, 1995, pp. 201–318.
- [7] T.A. Moore, A. Martinez, R.E. Tapscott, in: Proceedings of the 7th Halon Options Technical Working Conference, National Institute of Standards and Technology, 1997, pp. 388–395.
- [8] N. Saito, Y. Ogawa, Y. Saso, R. Sakai, Report of Fire Research Inst. of Japan, No. 81, 1996, pp. 22–29.
- [9] J.A. Senecal, in: Proceedings of the Central States Section Meeting. The Combustion Institute, 2004.
- [10] V.R. Katta, F. Takahashi, G. Linteris, in: *Fire Safety Science*: in: Proceedings of the Seventh International Symposium. International Association for Fire Safety Science, 2003, pp. 531–544.

Comments

James W. Fleming, *Naval Research Laboratory, USA*. 1. CF₃H acts primarily as a physical agent and there is a contribution to the non-catalytic H radical scavenging by the fluorine. The higher the extinction temperature of the CF₃H inhibited flame (higher than similar non-fluorine containing thermal agents) is likely due to the high exothermicity when HF is formed in the flame.

2. Pitts et al. [1] showed in counter-flow flames that where the heat is extracted in the flow field is essentially irrelevant. Based on your calculation, do you expect the same behavior in cup burner flames?

- [11] V.R. Katta, F. Takahashi, G. Linteris, *Combust. Flame* 137 (2004) 506–522.
- [12] G. Linteris, V.R. Katta, F. Takahashi, *Combust. Flame* 138 (2004) 78–96.
- [13] V.R. Katta, F. Takahashi, G. Linteris, *Combust. Flame* 144 (2005) 645–661.
- [14] F. Takahashi, G. Linteris, V.R. Katta, in: Proceedings of the 56th International Astronautical Congress. International Astronautical Federation, 2005.
- [15] F. Takahashi, G. Linteris, V.R. Katta, AIAA-2006-0745, 2006.
- [16] F. Takahashi, G. Linteris, V.R. Katta, *Proc. Combust. Inst.* 31 (2007) 1575–1582.
- [17] G. Linteris, F. Takahashi, V.R. Katta, in: Proceedings of the Halon Options Technical Working Conference (HOTWC), 2006.
- [18] W.M. Roquemore V.R. Katta, in: Proc. VSJ-SPIE98. Yokohama, Japan, Paper No. KL310, 1998.
- [19] M. Frenklach, H. Wang, M. Goldenberg, G.P. Smith, D.M. Golden, C.T. Bowman, R.K. Hanson, W.C. Gardiner, V. Lissianski, Technical Report No. GRI-95/0058, Gas Research Institute, Chicago, Illinois, 1995.
- [20] Anon., *NIST CKMech (Thermochemistry, Kinetics, Mechanisms)*, available at <http://fluid.nist.gov/ckmech.html>.
- [21] Anon., Computational Submodels, *International Workshop on Measurement and Computation of Turbulent Nonpremixed Flames*, available at <http://www.ca.sandia.gov/TNF/radiation.html>, 2003.
- [22] V.R. Katta, L.P. Goss, W.M. Roquemore, *AIAA J.* 32 (1994) 84.
- [23] B.J. McBride, M.J. Zehe, S. Gordon, NASA/TP—2002-211556, September 2002.
- [24] B.J. McBride, S. Gordon, NASA RP-1311, June 1996.
- [25] J. Warnatz, in: W.C. Gardiner (Ed.), *Combustion Chemistry*, Springer-Verlag, New York, 1984, pp. 197–360.
- [26] F. Takahashi, V.R. Katta, *Proc. Combust. Inst.* 30 (2005) 375–382.
- [27] R.W. Bilger, *Proc. Combust. Inst.* 22 (1988) 475.
- [28] F. Takahashi, V.R. Katta, *Proc. Combust. Inst.* 28 (2000) 2071–2078.

Reference

- [1] W.M. Pitts, J.C. Yang, M.L. Huber, L.G. Blevins, *Characterization and Identification of Super-Effective Thermal Fire Extinguishing Agents. First Annual Report*, NISTIR 6114, October 1999.

Reply. 1. Our calculations do not imply that CF₃H acts to extinguish cup-burner flames primarily through physical mechanisms. Plotting the extinguishing volume fraction of CF₃H versus the specific heat of the oxidizer stream (Fig. 3a) does show that the amount of CF₃H required for extinguishment is about the same as if it were

acting as a thermal diluent. Nonetheless, the essential parameter which would demonstrate physical (i.e., specific heat) influence on the flame is the temperature in the chain-branching region. Since the adiabatic flame temperature (Fig. 3b) and the calculated temperature in both the reaction kernel and in the trailing diffusion flame are all too high relative to those with added inert compounds, that action of CF_3H cannot be primarily thermal. Hence, as discussed in more detail in ([13] in the paper) [1,2], the action of CF_3H is primarily chemical (although a weaker chemical effect than with Br). Adding CF_3H increases the overall heat release in the flame, but simultaneously causes lower overall reaction rates because the radical volume fractions are much lower due to radical trapping by the fluorinated compounds.

2. Counterflow flames are essentially one-dimensional and steady, whereas cup-burner flames are at least two-dimensional and unsteady. The extinguishment of cup-burner flames, which are inherently low strain, occurs via a blow-off process rather than the global chemical extinction typical of counterflow diffusion flames. The reaction kernel in the flame base (edge) controls flame detachment, oscillation, and blow-off-type extinguishment [3]. Therefore, we would expect the cup-burner flames to be affected more by heat extraction in the reaction kernel than in other parts of the flame.

References

- [1] G.T. Linteris, L.F. Truett, *Combust. Flame* 105 (1996) 15–27.
- [2] G.T. Linteris, L.F. Truett, “Burning Rate of Premixed Methane-Air Flames Inhibited by Fluorinated Hydrocarbons,” *Halon Options Technical Working Conference*, Albuquerque, NM, May 3–5, 1994.
- [3] F. Takahashi, G. Linteris, V.R. Katta, *Proc. Combust. Inst.* 31 (2007) 1575–1582.

•

Bogdan Dlugogorski, The University of Newcastle, Australia. 1. There has been a tacit agreement among experimentalists that pressure does not affect the extinguishing concentration; e.g., in cases of experiments performed at locations where pressure is substantially below 1 atm. Do your modeling results support this agreement?

2. In the past, the adiabatic temperature at extinction has been used to gauge the importance of chemical suppression; i.e., higher adiabatic temperatures at extinction were taken to reflect the importance of chemical suppression. In your results, you show a high temperature for CF_3H , an agent that is not that active chemically during suppression. Please explain. Did you have a chance to measure by calcinate the concentration of HF at the outlet of your cup-burner apparatus?

Reply. 1. We have performed experiments and calculations of the minimum extinguishing concentration (MEC) of CO_2 in cup-burner flames in the oxidizer with the oxygen concentration of 21% (air) and 30% at 101 and 70.3 kPa, as described elsewhere [1]. Decreasing the atmospheric pressure decreased the MEC only moderately, whereas increasing the oxygen concentration significantly increased the MEC. Our calculations here show that, for physically acting agents, a threshold (≈ 1700 K) in the maximum flame temperature is a controlling factor in the cup-burner flame extinguishment. Because the effect of pressure on the flame temperature is small, compared to the oxygen concentration, its effect on the MEC is small as well.

2. This comment is addressed above in the previous response. Our results here indicate that CF_3H is active chemically in the flame, and this is described more completely in ([13] in the paper), which shows the inhibiting effect in cup-burner flames to be due to reduced radical volume fractions from reactions with F-containing compounds. Previous calculations and experiments for premixed flames indicated similar modes of action ([1,2] in above comment). In other work examining HF formation in suppressed flames ([6] in the paper), CF_3H was shown to completely decompose in premixed flames, forming COF_2 and HF commensurate with the amount of CF_3H added to the flame. Since participation in the relevant flame chemistry is necessary for HF formation, a purely physical mode of action for CF_3H is not consistent with our measurements of HF.

Reference

- [1] F. Takahashi, G. Linteris, V.R. Katta, AIAA-2006-0745, 2006.